Dynamics of arsenic adsorption in the targeted arsenic-safe aquifers in Matlab, south-eastern Bangladesh: Insight from experimental studies

Clare Robinson [a,b,*], Mattias von Brömssen [c,d], Prosun Bhattacharya [c], Sara Häller [c], Annelie Bivén [c], Mohammed Hossain [b,c], Gunnar Jacks [c], Kazi Matin Ahmed [e], M. Aziz Hasan [e], Roger Thunvik [c]

[a] Department of Civil and Environmental Engineering, University of Western Ontario, London, Canada N6A 5B9
[b] NGO Forum for Drinking Water Supply and Sanitation, Lalmatia, Dhaka 1207, Bangladesh
[c] KTH-International Groundwater Arsenic Research Group, Department of Land and Water Resources Engineering, Royal Institute of Technology, SE-100 44 Stockholm, Sweden
[d] Ramböll Sweden AB, Box 4205, SE-102 65 Stockholm, Sweden
[e] Department of Geology, University of Dhaka, Dhaka 1000, Bangladesh

ARTICLE INFO

ABSTRACT

Targeting shallow low-As aquifers based on sediment colour may be a viable solution for supplying As-safe drinking water to rural communities in some regions of Bangladesh and West Bengal in India. The sustainability of this solution with regard to the long-term risk of As-safe oxidized aquifers becoming enriched with As needs to be assessed. This study focuses on the adsorption behaviour of shallow oxidized sediments from Matlab Region, Bangladesh, and their capacity to attenuate As if cross-contamination of the oxidized aquifers occurs. Water quality analyses of samples collected from 20 tube-wells in the region indicate that while there may be some seasonal variability, the groundwater chemistry in the reduced and oxidized aquifers was relatively stable from 2004 to 2009. Although sediment extractions indicate a relatively low amount of As in the oxidized sediments, below 2.5 mg kg^{-1}, batch isotherm experiments show that the sediments have a high capacity to adsorb As. Simulations using a surface complexation model that considers adsorption to amorphous Fe(III) oxide minerals only, under-predict the experimental isotherms. This suggests that a large proportion of the adsorption sites in the oxidized sediments may be associated with crystalline Fe(III) oxides, Mn(IV) and Al(III) oxides, and clay minerals. Replicate breakthrough column experiments conducted with lactose added to the influent solution demonstrate that the high adsorption capacity of the oxidized sediments may be reduced if water drawn down into the oxidized aquifers contains high levels of electron donors such as reactive dissolved organic C.

© 2011 Elsevier Ltd. All rights reserved.

1. Introduction

Elevated concentrations of As in the groundwater of the shallow Holocene alluvial aquifers in the Bengal Delta Plain (BDP) of Bangladesh and West Bengal in India are a major health concern. Shallow hand tube-wells are the primary source of potable water in rural areas (BGS and DPHE, 2001; Bhattacharya et al., 2002a; Naidu and Bhattacharya, 2009). As a result, it is estimated that approximately 57 million people in Bangladesh currently drink water with As levels exceeding the World Health Organization (WHO) drinking water quality guideline of $10\,\mu g\,L^{-1}$ (Ahmed et al., 2004; Kapaj et al., 2006; Rahman et al., 2009; WHO, 2004). It is widely agreed that the elevated As concentrations are not attributable to anthropogenic activities and that the reductive dissolution of Fe(III) oxide minerals is the primary mechanism for release of adsorbed As to groundwater (Ahmed et al., 2004; Bhattacharya et al., 2006; Zheng et al., 2004; von Brömssen et al., 2007, 2008). In the BDP, As is derived naturally from sediments transported from the Himalayan range by the Ganges–Brahmaputra–Meghna river system. Elevated As concentrations are typically found in shallow tube-wells (<150 m) that are screened in the Holocene aquifers. Waters from tube-wells installed in the deeper Pleistocene aquifers generally have low As concentration (Ahmed et al., 2004; BGS and DPHE, 2001; Hasan et al., 2009; Polizzotto et al., 2005).

Tube-well switching and re-installation of tube-wells in As-safe sediments is strongly encouraged as an approach to provide safe drinking water supplies to rural communities (Jakariya et al., 2007; van Geen et al., 2002). The subsurface distribution of As is extremely heterogeneous, laterally and vertically, due to the complex hydrogeological and hydrogeochemical conditions in the BDP aquifers (Bhattacharya et al., 2006; Hasan et al., 2007). Although deeper aquifers typically have low dissolved As concentrations, the cost of installing deep tube-wells (>150 m) is often prohibitive.

* Corresponding author.
  E-mail address: crobinson@eng.uwo.ca (C. Robinson).

Identification of shallow aquifer sediments with low As concentrations that are suitable for placement of new tube-wells is needed to provide an affordable long-term safe drinking water option.

Previous studies have shown that redox conditions and dissolved As concentration are related to the colour of the aquifer sediment (Bhattacharya et al., 2010; Bundschuh et al., 2010; Jonsson and Lundell, 2004; von Brömssen et al., 2007, 2008). Overlying black–gray aquifer sediments tend to be reducing with high dissolved As levels. Off-white, yellowish and reddish sediments are oxidized with low risk of elevated As concentrations. In some areas, such as the Matlab Region, south-eastern Bangladesh, these oxidized sediments have been identified at shallow depths (<150 m) (Fig. 1) (von Brömssen et al., 2007, 2008). Targeting safe aquifers based on sediment colour may be a simple solution for delivering safe drinking water in this region and also in other regions where similar geological conditions exist. However, there is concern that tube-wells installed in As-safe sediments may become enriched in As over time. Water abstraction from the As-safe sediments may induce flow of reduced groundwater from surrounding sediments with high As concentration or surface water that is rich in electron donors such as dissolved organic C (DOC) to the As-safe aquifer zones (Polya and Charlet, 2009) to the safe aquifer zones (Fig. 2). While the oxidized sediments may initially have a high capacity to adsorb As, this capacity may be reduced by the increased availability of electron donors that stimulate the reduction of Fe(III) and Mn(IV) oxides (Bhattacharya et al., 2009; Sharif et al., 2008; Stollenwerk et al., 2007). The reduction of these minerals may lead to the transfer of sediment-bound As to the groundwater. An increased availability of ions that compete with As for adsorption sites (e.g., PO_4^{3-}, Si, Ca, HCO_3^-) may also stimulate the release of sediment-bound As (Nath et al., 2009; Polya and Charlet, 2009). Understanding of the adsorption behaviour of the oxidized sediments and their ability to attenuate As if cross-contamination occurs is, therefore, needed to evaluate the sustainability of targeting the shallow As-safe sediments. Although prior studies have examined the processes leading to As mobilization in the reduced sediments, there is limited understanding of the adsorption processes in the oxidized sediments.

The objective of this study is to investigate the adsorption dynamics of the oxidized sediments. Water chemistry analyses conducted for tube-wells installed in the reduced and oxidized aquifers in the Matlab Region from 2004 to 2009 are first presented. The adsorption characteristics of the oxidized sediments are then investigated by (1) sediment extractions; (2) batch As adsorption isotherm experiments combined with geochemical modeling; and (3) breakthrough column tests examining the influence of DOC on the As adsorption capacity of the sediments.

2. Materials and methods

2.1. Study site

The villages of North Digaldi and Mobarakdi in the Matlab Region of the Chandpur District, approximately 60 km SE of Dhaka were selected as the study area (Fig. 1). Matlab Region has pronounced levels of As-enrichment with approximately 70% of the total functional tube-wells ($n \approx 13,000$) measured to have As concentrations exceeding the WHO guideline value of 10 $\mu g\,L^{-1}$ (Jakariya et al., 2007). The surface geology of the Matlab Region is generally divided into an upper reduced aquifer and a lower oxidized aquifer with representative sediment colours. However, the subsurface distribution of As however is extremely heterogeneous with strong local variability in the hydrogeology and geochemistry. In some locations the reduced and oxidized aquifers are separated by a clay aquitard at a depth of ~30–50 m, but this layer is not continuous. Historically, tube-wells in the study area were installed in both aquifers. Analyses indicate that the As-unsafe tube-wells are primarily those located in the reduced sediments (von Brömssen et al., 2007, 2008). Re-installation of As-unsafe tube-wells in shallow oxidized As-safe sediment with local drillers targeting these aquifers based on sediment colour may be a sustainable low cost mitigation solution for supplying As-safe drinking water in this region.

2.2. Sample collection and analysis

Hand tube-wells ($n = 20$) installed in oxidized and reduced aquifers were sampled in April–May 2004, January 2005, November 2006, January 2008 and March–April 2009 to identify temporal water quality variations and to provide water chemistry data for the laboratory experiments. Water quality results for these tube-wells for April–May 2004 have been previously reported by von Brömssen et al. (2007). For all sampling events two water samples were collected from each tube-well: a 60 mL filtered sample for major anion analysis and a 60 mL filtered sample acidified with 7 M supapure HNO_3 for analysis of cations and trace elements including As (Bhattacharya et al., 2002b). Basic physiochemical parameters (dissolved O_2, temperature, pH and Eh) were measured in the field for all tube-wells using a flow through cell following the procedures described by Bhattacharya et al. (2002b). Field speciation of As(III) was carried out using a Disposable Cartridge® (Meng et al., 2001) with the samples acidified and transported to the laboratory for analysis. The concentration of As(V) was estimated by calculating the difference between total As and As(III) in sample. Two boreholes (A and B) were drilled in North Dighaldi and Mubarakdi villages during November 2006 to collect oxidized sediment samples for the laboratory experiments and to compare the sediment lithology with that previously reported by von Brömssen et al. (2007). Sediment samples were collected every
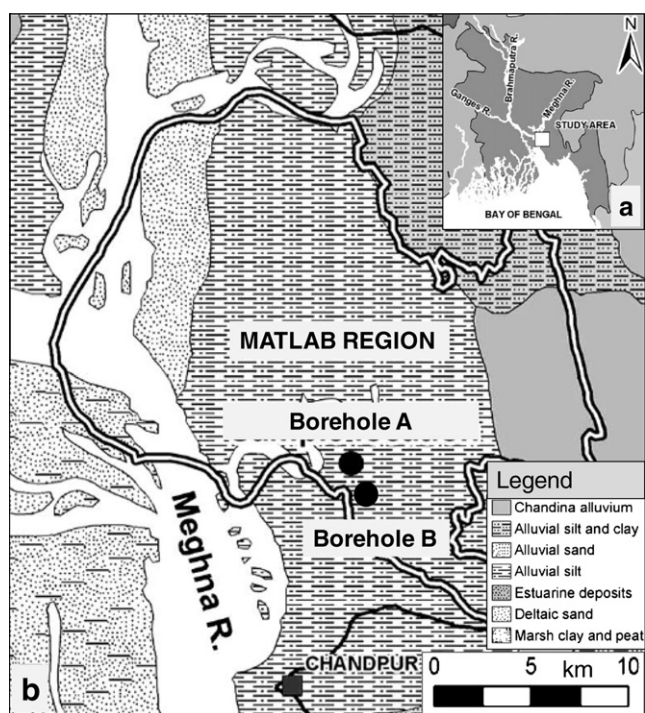

Fig. 1. (a) Location of Matlab Region in south-eastern Bangladesh, and (b) location of site boreholes drilled within Matlab Region (modified from von Brömssen et al., 2008).
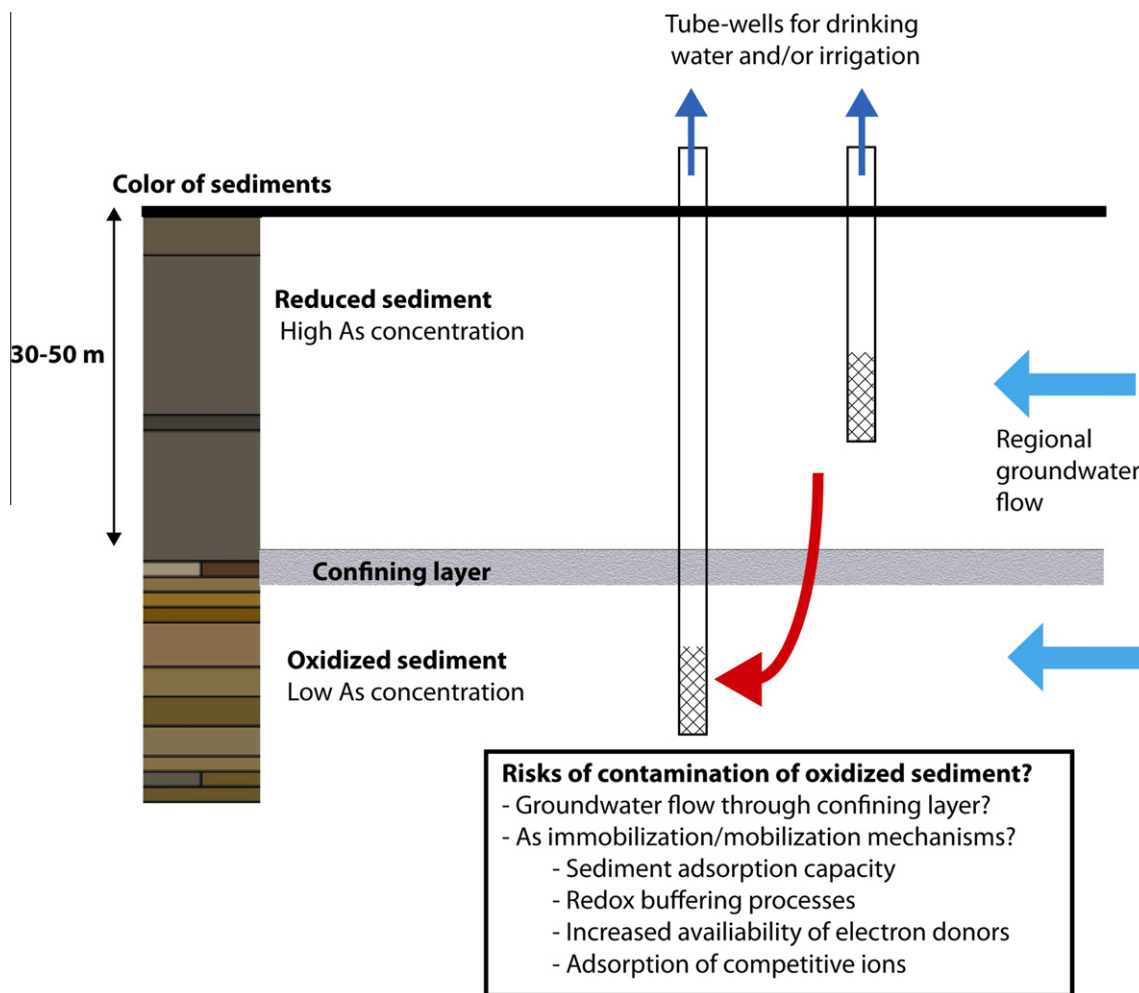
Fig. 2. Conceptual diagram of the risks of As-enrichment of the oxidized aquifer in Matlab Region, south-eastern Bangladesh.

∼1.5 m to a total depth of ∼60 m. The colour and texture of each sample was recorded.

Alkalinity of the water samples was measured according to the standard method SS-EN ISO 9963-2 (SIS, 1996) by titrating the filtered unacidified water samples with HCl. Major anions were determined with a Dionex DX-120 ion chromatograph with an Ion-Pac As9-SC column. Major cations and trace elements were determined by inductively coupled plasma (ICP) emission spectrometry. Ammonium and total PO_4^{3-} were quantified using a Tecator Aqua-Tec 5400 analyser with flow injection analysis. DOC was measured using a Shimadzu 5000 TOC analyser ($0.5\ mg\ L^{-1}$ detection limit with ±10% precision).

2.3. Laboratory experiments

Geochemical and adsorption characteristics of the oxidized sediments were investigated by extractions, batch isotherm experiments, and column experiments. Three sediment samples with distinct oxidized colour and from locations below the clay aquitard were selected for these experiments. Samples #1 and #3 were from borehole A at depths of 48.8 m and 53.3 m, respectively, and Sample #2 was from borehole B at a depth of 51.8 m. Extractions with 0.2 M oxalate ($NH_4C_2O_4$) solution were conducted for each sediment sample to quantify the elements, including Fe, Mn and Al, present as amorphous oxides and hydroxides. Extractions with 7 M HNO_3 were also conducted to quantify the amounts of As and other elements associated with the non-silicate minerals

(i.e., including crystalline phases). Duplicates were performed for each sample. The procedure for these extractions is detailed in Bivén and Häller (2007).

Batch adsorption isotherm tests were conducted using the three sediment samples. For each sample, 2 g of drained sediment was mixed with 30 mL 0.01 M $NaNO_3$ in centrifuge tubes. Sodium hydroxide (NaOH) and HNO_3 were added to adjust the pH to 7. Distilled water with 7 different concentrations of As(V) ranging from 0.2 to $100\ mg\ L^{-1}$ (added as K_2HAsO_4) were then added to each sediment sample, giving 21 filled centrifuge tubes. The tubes were placed in a vertical rotating shaker for 2 weeks and then the samples were centrifuged and filtered. Considering the thermodynamic stability of As and Fe in the oxidized sediments, As(V) was used for the batch tests because it was considered to be the predominant sediment-bound As species in the oxidized aquifers. Dissolved As was very low in most of the groundwater samples abstracted from the oxidized aquifers with no detectable As(III) (Table 3).

Column experiments were conducted to examine the influence of DOC on the adsorption capacity of the oxidized sediments. Six columns, each with a diameter of 2 cm and height of 10 cm, were filled with 45 g of oxidized sediments. Two identical columns for each of the three oxidized sediment samples were set up. Distilled water, prepared with NaCl, $NaHCO_3$ and $NaAsO_2$, was leached through the columns. The concentrations of As, Na, Cl and alkalinity in the influent water correspond to the mean measured concentrations in groundwater from tube-wells in the reduced sediments in Matlab Region in November 2006 (Table 3). Data from this

sampling event was used as this corresponds to the time the sediment samples were collected. Arsenic(III) was used in the influent water as it is the major As redox species in the reduced ground waters in the BDP and the Matlab Region (Table 3), and thus in the water that will infiltrate into the oxidized aquifers (Ahmed et al., 2004). In the replicate columns, 0.2 wt.% lactose was added to the influent solution to stimulate the reductive dissolution of Fe(III) and Mn(IV) oxides. Prior to the addition of the chemicals the influent water was bubbled with N_2 to remove any dissolved O_2. The flow rate through the columns was adjusted to 2 mL day^{-1} and the experiments were run for 13 weeks. The concentrations of major anions, cations and trace elements was in the influent and effluent solutions were determined once a week through the experimental period. The quantity of As adsorbed was calculated as the difference between the influent and effluent As concentrations.

2.4. Geochemical modeling

The adsorption of As on the oxidized sediments was simulated as surface complexation reactions on generic hydroferric oxides (Hfo) surfaces using the Diffuse Layer Model of Dzombak and Morel (1990). The modeling was conducted using the geochemical modeling platform PHREEQC (Parkhurst and Appelo, 1999). The Minteq.v4 (Allison et al., 1990) database was adopted and modified as required. Using the surface complexation approach the adsorption of species to Hfo are described by equilibrium mass action equations. The Dzombak and Morel (1990) model includes both strong and weak binding sites on Hfo. The surface reactions considered and thermodynamic constants used are provided in Table 1.

The surface composition (i.e., concentration of adsorbed species) of the oxidized sediments in equilibrium with the mean field water chemistry in November 2006 was first simulated. The surface complexation model adopted assumes that amorphous Fe(III) oxides are the dominant mineral adsorbent phase compared with amorphous Mn(IV) and Al(III) oxides and any crystalline and clay minerals (Sharif et al., 2008; von Brömssen et al., 2008). The simulated adsorbed As (and other adsorbent species shown in Table 1) depends strongly on the reactions and thermodynamic constants used and surface assemblage (number of strong and weak adsorption sites and Hfo surface area) adopted. From Dzombak and Morel (1990), a specific surface area (600 m^2 g^{-1}) and site densities of 0.2 mol weak sites/mol Hfo and 0.005 mol strong sites/mol Hfo were used. The model input data are provided in Table 2. Hfo abundance simulated was calculated from the Fe released from amorphous minerals by the oxalate extraction (Fe$_{ox}$). The modeling approach (including reactions and constants considered) was validated by comparing the simulated surface composition with that measured from the oxalate extraction. The saturation indices for aquifer minerals were also calculated to identify the possible sinks and sources of dissolved species in the oxidized aquifer.

The PHREEQC model was then applied to simulate the measured experimental adsorption isotherms and test the extent to which the model, which considers adsorption to amorphous Fe(III) oxides only, could predict the adsorption behaviour of the sediment. The initial surface composition was simulated to be that in equilibrium with the mean field water chemistry in the oxidized sediments in November 2006. This surface composition was then equilibrated with each batch experiment solution.

3. Results and discussion

3.1. Water chemistry

Major water chemistry data for the 20 sampled tube-wells for the five sampling events is provided in Table 3 with a summary

Table 1
Reactions and thermodynamic constants for PHREEQC surface complexation model with strong (Hfo_s) and weak (Hfo_w) adsorption sites.

Adsorption reaction	Log K	Reference
$Hfo\_sOH + H^+ = Hfo\_sOH_2^+$	7.29	Allison et al. (1990)
$Hfo\_wOH + H^+ = Hfo\_wOH_2^+$	7.29	
$Hfo\_sOH = Hfo\_sO^- + H^+$	−8.93	
$Hfo\_wOH = Hfo\_wO^- + H^+$	−8.93	
Arsenite		
$Hfo\_sOH + H_3AsO_3 = Hfo\_sH_2AsO_3 + H_2O$	5.41	Allison et al. (1990)
$Hfo\_wOH + H_3AsO_3 = Hfo\_wH_2AsO_3 + H_2O$	5.41	
Arsenate		
$Hfo\_sOH + H_3AsO_4 = Hfo\_sH_2AsO_4 + H_2O$	8.61	Allison et al. (1990)
$Hfo\_wOH + H_3AsO_4 = Hfo\_wH_2AsO_4 + H_2O$	8.61	
$Hfo\_sOH + H_3AsO_4 = Hfo\_sHAsO_4^- + H_2O + H^+$	2.81	
$Hfo\_wOH + H_3AsO_4 = Hfo\_wHAsO_4^- + H_2O + H^+$	2.81	
$Hfo\_sOH + H_3AsO_4 = Hfo\_sOHAsO_4^{-3} + 3H^+$	−10.12	
$Hfo\_wOH + H_3AsO_4 = Hfo\_wOHAsO_4^{-3} + 3H^+$	−10.12	
Phosphate		
$Hfo\_sOH + PO_4^{-3} + 3H^+ = Hfo\_sH_2PO_4 + H_2O$	31.29	Allison et al. (1990)
$Hfo\_wOH + PO_4^{-3} + 3H^+ = Hfo\_wH_2PO_4 + H_2O$	31.29	
$Hfo\_sOH + PO_4^{-3} + 2H^+ = Hfo\_sHPO_4^- + H_2O$	25.39	
$Hfo\_wOH + PO_4^{-3} + 2H^+ = Hfo\_wHPO_4^- + H_2O$	25.39	
$Hfo\_sOH + PO_4^{-3} + H^+ = Hfo\_sPO_4^{-2} + H_2O$	17.72	
$Hfo\_wOH + PO_4^{-3} + H^+ = Hfo\_wPO_4^{-2} + H_2O$	17.72	
Carbonate		
$Hfo\_wOH + CO_3^{-2} + H^+ = Hfo\_wCO_3^- + H_2O$	12.56	van Geen et al. (2004)
$Hfo\_wOH + CO_3^{-2} + 2H^+ = Hfo\_wHCO_3 + H_2O$	20.62	
Silica		
$Hfo\_sOH + H_4SiO_4 = Hfo\_sH_3SiO_4 + H_2O$	4.28	Swedlund and Webster (1999)
$Hfo\_wOH + H_4SiO_4 = Hfo\_wH_3SiO_4 + H_2O$	4.28	
$Hfo\_sOH + H_4SiO_4 = Hfo\_sH_2SiO_4^- + H_2O + H^+$	−3.22	
$Hfo\_wOH + H_4SiO_4 = Hfo\_wH2SiO_4^- + H_2O + H^+$	−3.22	
$Hfo\_sOH + H_4SiO_4 = Hfo\_sHSiO_4^{-2} + H_2O + 2H^+$	−11.69	
$Hfo\_wOH + H_4SiO_4 = Hfo\_wHSiO_4^{-2} + H_2O + 2H^+$	−11.69	
Calcium		
$Hfo\_sOH + Ca^{2+} = Hfo\_sOHCa^{2+}$	4.97	Allison et al. (1990)
$Hfo\_wOH + Ca^{2+} = Hfo\_wOCa^+ + H^+$	−5.85	

of key parameters presented in Fig. 3. Samples from tube-wells installed in reddish, yellow, off-white and white sediments are categorized as from an oxidized aquifer layer. Samples from tube-wells installed in grayish-black sediments are categorized as from a reduced aquifer layer (von Brömssen et al., 2007). The groundwater samples are neutral to slightly acidic for both sediment types (Fig. 3). For all sampling events, groundwater from the reduced sediments is characterized by high total As, DOC, Fe, PO$_4^{3-}$ and low Mn concentrations. The major aqueous As redox species is As(III) in the water samples from the reduced sediments. The groundwater from the oxidized sediments is characterized by high Mn and low total As, DOC, Fe, and PO$_4^{3-}$ concentrations. Where total As was detected, As(III) was below detection limits for all samples except two. This indicated that As(V) is the major As redox species in the water samples from the oxidized sediments. The high Mn and low Fe concentrations in the water samples from the oxidized sediments indicate that the redox state is such that Mn(IV) oxides have been reduced, but it is not sufficiently low for the reduction of Fe(III) oxides. In contrast, the elevated Fe in the groundwater from the reduced sediments indicates that reductive dissolution of Fe(III) oxides occurs in these sediments. Based on the redox sequence, reduction of Mn(IV) oxides would also have occurred in the reduced sediments. However, dissolved Mn levels in these sediments are low, and this is likely because the concentration of Mn(II) is controlled by the precipitation of Mn(II) minerals (e.g., rhodochrosite and MnHPO$_4$) (von Brömssen et al., 2008). While DOC concentrations are higher in the reduced compared with the

Table 2
Input parameters for PHREEQC surface complexation model.

	Sample #1	Sample #2	Sample #3	Comments
Input data for simulations of oxidized aquifer conditions				
Hfo (g L^{-1})	0.9	0.79	0.66	Calculated from oxalate extraction
Weak sites (sites L^{-1})	2×10^{-3}	1.8×10^{-4}	1.4×10^{-3}	Used Dzombak and Morel (1990) site density of 0.2 sites/ mol Hfo and molecular weight Hfo = 88.8 g mol^{-1}
Strong sites (sites L^{-1})	5×10^{-5}	4.5×10^{-5}	3.5×10^{-5}	Used Dzombak and Morel (1990) site density of 0.005 sites/mol Hfo
Liquid/Solid ratio (L kg^{-1})	0.238	0.238	0.238	To convert between aquifer and experimental conditions. Based on porosity = 0.3 and bulk sediment density = 1.8 kg L^{-1}

oxidized sediments, the type and reactivity of the DOC was not established.

Consistent with previous studies there is strong correlation between the sediment type and dissolved As concentration (Fig. 3). Waters extracted from the oxidized sediments typically have As concentrations below the WHO guideline value of 10 µg L^{-1} (WHO, 2004). Concentrations of As in water samples from the reduced sediments vary from <50 to 400 µg L^{-1}. Low As concentrations in the oxidized sediments may be because, compared with the reduced sediments, adsorption sites are not saturated due to a higher abundance of Fe(III) and Mn(IV) oxides. Phosphate also has a high adsorption capacity and the low dissolved PO$_4^{3-}$ concentrations in the oxidized sediments may also be due to the higher abundance of oxide minerals.

The water chemistry for the tube-wells is relatively stable over the sampling years (2004–2009) with some exceptions. The As concentrations were 1.1–3.0 times higher in 15 of the tube-wells (installed in both the oxidized and reduced sediments) in November 2006 compared with the other sampling events. This fluctuation may be associated with seasonal variability. The monsoon season in Bangladesh occurs from June to October. In 2006 the sampling was undertaken post-monsoon (November), in contrast to other years when samples were collected before the monsoon (January–May). Infiltration of organic-rich waters during the monsoon, as suggested by increased DOC levels in the oxidized sediments, may account for the higher As concentrations in November 2006. For the tube-wells in the reduced sediments, the January 2008 data show an increase in the mean total Mn concentrations and decrease in Fe concentrations, suggesting Mn and Fe cycling. Concentrations of As in water samples from the reduced sediments also increased slightly in January 2008 compared with January 2005. If reductive dissolution of Fe(III) oxides is controlling As mobilizations, the increase in As is not consistent with the decrease in dissolved Fe concentrations also observed. This may be because once reduced Fe(II) is sequestered in solid phases such as siderite, Fe(II) sulfide and vivianite. Longer-term water quality measurements, including monthly tube-well sampling and correlation with climatic factors such as rainfall, is required to better understand the temporal variability in As concentrations.

The sediment sequences for the two boreholes drilled in November 2006 are consistent with those observed by von Brömssen et al. (2007) (Fig. 4). The lithologs show a distinct clay aquitard at both locations at

a depth of around 30–50 m. The sediments below the aquitard were primarily yellowish-red in colour and those above were greyish-black. Characterization of the oxidized and reduced sediments in Matlab Region was conducted previously by von Brömssen et al. (2008). Their analyses indicated that the greyish-black (reduced) sediments have a higher content of amorphous Fe(III) and Mn(IV) oxides compared with the off-white and yellowish (oxidized) sediments where Fe(III) and Mn(IV) are present as more crystalline phases.

3.2. Arsenic adsorption dynamics

3.2.1. Extractions

Oxalate and HNO$_3$ extractions performed on the three oxidized sediment samples (Sample #1, Sample #2 and Sample #3) indicate that the content of As associated with the solid phase is relatively low. The As content was measured to be <1.3 mg kg^{-1} and between 1.3 and 2.4 mg kg^{-1} by the oxalate and HNO$_3$ extractions, respectively (Table 4). The oxalate extractions indicate that the content of Fe associated with the amorphous fraction (Fe$_{ox}$) is between 94 and 134 mg kg^{-1}, and that associated with the crystalline fraction is considerably higher (5070–6940 mg kg^{-1}). This result is in agreement with von Brömssen et al. (2008) who showed that the fractions of amorphous Fe and Mn phases are low compared to the crystalline fractions for the oxidized sediments. From observing changes in sediment colour during extractions, von Brömssen et al. (2008) noted that the reddish colour of the oxidized sediment is primarily associated with the crystalline minerals.

The surface composition of the oxidized sediments was simulated in PHREEQC using the November 2006 mean water chemistry data for tube-wells installed in the oxidized sediments. The Hfo mass and surface site concentrations were derived from Fe$_{ox}$ (Table 2). The model gives a good match between the predicted concentration of adsorbed species and those extracted from the amorphous minerals (Fig. 5). The adsorption of As relative to other ions that compete for adsorption sites is also consistent. For all samples the quantity of adsorbed As is predicted to be ~1 mg kg^{-1}. The model assumes that As is present as As(V). The relative quantity of adsorbed As predicted is similar regardless of whether As(III) or As(V) is considered. The discrepancy between the simulated and measured surface composition may be attributed to varying water chemistry at the specific location from where the sediment was collected and/or influence of other amorphous adsorbing phases including Al(III) and Mn(IV) oxides which are not considered in the model. The reasonable match between the experimental and simulated data suggests that the competitive adsorption of As with Ca, Si, CO$_3^{2-}$ and PO$_4^{3-}$ ions is well represented by the surface reactions and parameter values adopted (Table 1). Calculated saturation indices indicate that the groundwater in the oxidizing sediments is supersaturated with respect to Fe(III) and Al(III) oxide minerals including ferrihydrite (Fe(OH)$_3$), geothite (FeOOH), magnetite (Fe$_3$O$_4$) and gibbsite (Al(OH)$_3$). This suggests potential for the precipitation of these minerals and therefore increased availability of adsorption sites. The groundwater is also slightly supersaturated with respect to MnHPO$_4$ (SI = 1.72). von Brömssen et al. (2008) suggest that the solubility of MnHPO$_4$ may control the availability of dissolved PO$_4^{3-}$ that competes with As for adsorption sites.

3.2.2. Adsorption isotherms

The sustainability of targeting the oxidized sediments as a source of As-safe drinking water is influenced by the capacity of these sediments to attenuate As in groundwater that may flow in from As-rich reduced aquifer sediments. Adsorption isotherms were generated for the three oxidized sediment samples by combining the sediments with solutions with low (0.2–1 mg L^{-1}) and high (5–100 mg L^{-1}) As(V) concentrations. The quantity of

Table 3
Water chemistry data for tube-wells installed in oxidized and reduced sediments in South Matlab.

ID	Location	Sediment colour	Sampling date	Depth (m)	Temp (°C)	pH	Eh (mV)	EC (μS cm⁻¹)	HCO$_3$ (mg L⁻¹)	SO$_4$ (mg L⁻¹)	Cl (mg L⁻¹)	NO$_3$–N (mg L⁻¹)	PO$_4$–P (mg L⁻¹)	Na (mg L⁻¹)	K (mg L⁻¹)	Mg (mg L⁻¹)	Ca (mg L⁻¹)	Total As (μg L⁻¹)	As(III) (μg L⁻¹)	Total Fe (mg L⁻¹)	Total Mn (mg L⁻¹)	Si (mg L⁻¹)	DOC (mg L⁻¹)
Oxidized sediment																							
A	North Dighaldi	Off-white	11-May-04	57.9	26.8	6.12	346	1038	107	1.01	255	0.20	0.21	75.9	4.2	25.8	53.8	<DL	<DL	0.13	2.53	53.0	0.53
			30-January-05		26.2	6.27	162	1024	106	5.12	233	0.85	0.17	88.1	3.8	23.9	57.1	<DL	<DL	0.28	2.59	48.8	0.91
			29-November-06		25.8	6.40	297	910	103	4.40	234	0.43	0.16	82.3	3.4	24.9	58.8	16	<DL	0.32	2.62	34.8	0.80
			18-January-08		25.6	6.34	294	952	102	3.97	245	<DL	0.09	90.1	3.9	23.2	57.0	<DL	<DL	0.26	2.54	43.2	4.92
			14-March-09		26.1	6.50	77	910	125	2.41	267	1.23	0.06	77.0	2.0	24.4	62.2	9	<DL	0.40	1.51	18.9	1.29
B	Mobarakdi	Red	11-May-04	57.9	26.6	6.39	304	777	136	0.44	149	0.23	0.35	54.3	3.4	20.8	43.1	<DL	<DL	0.32	1.99	43.7	1.01
			30-January-05		25.6	6.59	159	801	154	1.44	150	0.20	0.07	59.9	2.4	20.2	53.9	<DL	<DL	0.79	2.04	39.9	0.36
			28-November-06		25.0	6.60	290	710	147	1.30	147	0.23	0.06	54.7	2.3	21.4	56.7	13	<DL	0.81	2.04	29.8	1.35
			18-January-08		24.8	6.76	286	710	151	1.35	152	0.01	0.10	53.7	2.5	26.3	50.8	<DL		0.72	2.12	37.7	1.82
16	North Dighaldi	Red	27-May-04	61	26.7	6.17	387	936	96	4.08	206	0.49	0.29	62.4	3.6	24.4	53.0	<DL	<DL	0.36	3.19	49.1	1.41
			30-January-05		26.1	6.14	191	909	117	4.47	185	0.30	0.17	61.1	3.2	22.3	62.5	<DL	<DL	0.37	3.16	44.5	0.56
			29-November-06		26.2	6.40	331	770	108	4.40	187	0.65	0.12	60.7	2.9	22.6	57.5	11	<DL	0.70	3.14	32.3	0.78
			18-January-08		23.5	6.47	267	791	116	4.24	189	<DL	0.15	59.6	3.3	23.1	60.4	6	<DL	1.00	3.27	43.8	1.68
19	North Dighaldi	Off-white	29-April-04	59.4	26.5	6.20	281	1042	112	0.59	232	1.00	0.14	78.8	3.6	26.5	53.2	<DL	<DL	0.20	3.58	50.2	0.54
			30-January-05		26.2	6.29	263	1050	116	0.62	230	0.39	0.10	80.8	3.2	23.0	57.9	<DL	<DL	0.21	3.53	43.2	0.65
			29-November-06		26.2	6.50	298	890	124	0.60	216	1.12	0.08	76.2	2.9	25.1	60.6	8	<DL	0.18	3.61	32.1	0.67
20	North Dighaldi	Off-white	29-April-04	59.4	26.7	6.19	255	891	107	3.25	220	0.54	0.33	58.4	3.7	22.4	59.7	<DL	<DL	0.41	2.90	54.7	0.47
			30-January-05		26.3	6.32	297	995	87	4.76	230	0.27	0.20	78.6	3.3	21.6	56.8	<DL	<DL	0.27	3.01	43.7	0.53
			29-November-06		26.9	6.30	313	860	95	4.50	216	0.82	0.20	75.2	3.0	22.1	60.0	7	<DL	0.43	3.21	32.7	0.86
			18-January-08		25.3	6.45	304	881	100	4.40	230	<DL	0.18	81.8	3.5	21.9	60.5	6	<DL	0.24	3.15	41.1	2.73
			14-March-09		26.7	7.0		830	105		232	0.95	0.08	81.8	2.9	26.0	68.5	8	<DL	0.23	4.30	26.6	1.74
26	Mobarakdi	Red	29-April-04	53.3	26.5	6.19	294	815	113	2.34	169	0.51	0.39	55.2	3.3	21.1	45.5	<DL	<DL	0.24	2.34	53.6	1.00
			30-January-05		26.1	6.30	273	809	112	3.07	168	0.20	0.23	58.7	3.1	19.6	48.8	<DL	<DL	0.27	2.35	48.9	0.60
			28-November-06		25.1	6.40	295	720	114	2.80	167	0.94	0.24	54.7	3.0	21.5	55.0	6	<DL	0.42	2.40	35.0	0.97
			18-January-08		26.2	6.59	295	729	112	2.23	170	<DL	0.21	60.0	3.1	20.9	51.1	<DL	<DL	0.42	2.32	41.9	2.11
32	Mobarakdi	Red	30-April-04	64.0	26.8	6.38	298	795	140	3.81	150	1.01	0.21	59.5	3.4	19.0	49.6	<DL	<DL	0.37	3.96	46.3	1.18
			30-January-05		26.3	6.40	240	860	141	0.15	156	0.22	0.09	63.4	3.1	19.1	49.7	<DL	<DL	0.37	3.68	41.0	0.73
			28-November-06		29.1	6.50	284	700	136	<DL	156	0.52	0.08	60.5	2.8	20.2	50.4	10	<DL	0.47	3.81	31.5	0.79
			18-January-08		25.9	6.72	318	716	142	0.45	154	<DL	0.08	66.7	3.1	20.0	48.7	<DL	<DL	0.36	3.50	37.9	2.72
35	Mobarakdi	Off-white	30-April-04	79.3	26.8	6.33	256	925	118	0.96	199	0.39	0.20	68.6	3.9	24.1	47.7	<DL	<DL	0.33	2.57	55.8	0.93
			30-January-05		26.2	6.31	226	957	128	0.56	168	0.30	0.11	74.4	3.6	22.7	54.9	<DL	<DL	0.29	2.67	50.0	0.32
			28-November-06		25.3	6.60	240	810	126	<DL	196	0.60	0.11	67.4	3.2	23.4	58.7	<DL	<DL	0.45	2.69	36.0	0.80
			18-January-08		25.8	6.68	310	889	125	0.75	204	<DL	0.10	75.6	3.7	22.9	56.0	<DL	<DL	0.40	2.72	46.6	0.85
			13-March-09		26.8	7.10	289	820	126	2.33	309	1.23	0.05	75.5	3.0	26.6	64.2	<DL	<DL	0.30	3.71	30.7	1.25
44	Mobarakdi	White	3-May-04	57.9	26.8	6.77	152	1652	415	<DL	272	1.22	3.93	202.1	4.7	34.0	62.8	37	35.8	7.06	0.22	39.0	1.95
			30-January-05		26.5	6.73	113	1662	402	0.15	268	1.15	3.94	223.8	4.4	29.4	72.0	43	44.7	7.06	0.24	36.4	2.66
			29-November-06		26.1	6.70	221	1370	383	<DL	264	0.54	3.67	205.1	3.8	29.2	68.3	64		6.97	0.25	26.7	2.09
			19-January-08		24.8	6.84	337	1428	401	<DL	276	0.24	3.16	192.4	4.5	36.3	67.5	52	10.1	6.92	0.27	33.8	3.20
			5-April-09		26.6	7.50	207	1470	410	0.18	266	<DL	3.80	210.1	3.5	32.2	80.2	42	35.5	8.22	0.28	21.3	3.02
51	Mobarakdi	Off-white	30-April-04	57.9	26.7	6.66	272	2420	355	3.71	530	0.98	0.56	374.7	4.1	28.7	57.1	<DL	<DL	0.14	1.93	32.2	0.65
			30-January-05		26.5	6.62	249	2450	350	4.91	526	2.51	0.37	378.7	3.6	25.3	62.0	<DL	<DL	0.13	1.91	28.8	0.81
			30-November-06		24.0	6.70	263	1910	344	5.62	518	1.65	0.41	370.3	3.4	25.8	62.7	<DL	<DL	0.29	1.93	23.0	0.89
			19-January-08		22.9	6.71	320	1920	350	4.03	515	<DL	0.31	380.5	3.6	33.4	60.3	<DL	<DL	0.47	1.76	26.6	2.35
			5-April-09		26.3	6.0	274	2060	394	5.97	852	1.72	0.15	290.4	2.5	25.6	61.4	9	<DL	0.12	1.90	14.3	1.55
58	Mobarakdi	Off-white	1-May-04	57.9	26.8	6.66	211	2800	319	4.62	648	1.51	1.58	400.4	4.7	40.4	77.7	19	19.1	2.06	1.76	30.9	0.68
			30-January-05		26.3	6.69	184	2830	292	8.40	653	0.47	1.31	432.6	4.3	32.3	86.9	27	24.5	2.05	1.78	27.6	1.27
			29-November-06		24.9	6.70	263	2760	311	5.44	603	<DL	1.42	388.0	4.7	34.6	79.7	35	<DL	2.47	1.74	22.3	0.83
			19-January-08		24.3	6.87	293	2410	318	3.93	638	<DL	1.30	362.0	4.5	41.3	79.8	34	9.4	2.74	1.76	27.0	3.42
			4-April-09		27.0	7.40	297	2350	353	7.01	256	0.94	1.44	344.0	3.4	36.9	90.9	44	34.3	2.62	2.17	16.8	1.62
63	Mobarakdi	Red	1-May-04	68.6	26.6	6.51	294	1971	166	<DL	486	1.23	0.22	208.5	6.1	42.2	94.0	<DL	<DL	0.34	2.16	35.6	1.00
			30-January-05		26.1	6.50	262	2000	166	0.15	484	0.66	0.16	221.7	5.4	34.7	93.4	<DL	<DL	0.43	2.21	32.1	0.68
			28-November-06		26.9	6.60	269	1740	165	<DL	493	<DL	0.15	209.4	4.8	37.2	92.0	7	<DL	0.81	2.36	24.7	1.94
			19-January-08		24.9	6.62	309	1791	166	<DL	521	0.54	0.13	210.7	6.0	38.7	93.8	<DL	<DL	0.81	2.36	31.0	2.98
			6-April-09		26.7	6.60	327	1820	187	0.16	469	1.75	0.10	232.9	4.9	46.6	119.4	10	<DL	0.81	3.32	20.8	

Table 3 (continued)

ID	Location	Sediment colour	Sampling date	Depth (m)	Temp (°C)	pH	Eh (mV)	EC (μS cm⁻¹)	HCO₃ (mg L⁻¹)	SO₄ (mg L⁻¹)	Cl (mg L⁻¹)	NO₃-N (mg L⁻¹)	PO₄-P (mg L⁻¹)	Na (mg L⁻¹)	K (mg L⁻¹)	Mg (mg L⁻¹)	Ca (mg L⁻¹)	Total As (μg L⁻¹)	As(III) (μg L⁻¹)	Total Fe (mg L⁻¹)	Total Mn (mg L⁻¹)	Si (mg L⁻¹)	DOC (mg L⁻¹)
Reduced sediment																							
25	Mobarakdi	Black	30-April-04	24.4	26.1	6.81	128	840	307	0.15	83	0.62	7.28	102.3	6.2	17.0	36.1	241	241.0	6.77	0.13	43.1	3.79
			30-January-05		25.8	7.00	121	874	305	0.15	110	0.46	7.55	104.9	5.7	17.2	40.6	269	259.4	6.92	0.14	39.8	4.67
			28-November-06		22.6	7.00	308	800	301	<DL	94	0.58	6.79	95.0	5.0	19.1	50.9	383	108.7	7.54	0.16	29.8	5.37
			18-January-08		23.0	6.85	305	743	303	<DL	86	0.74	6.96	89.4	5.8	22.3	42.8	323		7.04	0.18	37.4	4.01
37	Mobarakdi	Black	1-May-04	39.6	26.8	6.58	176	1598	189	<DL	356	1.00	3.64	189.0	5.3	25.3	51.4	19	23.2	9.18	0.28	52.3	1.05
			30-January-05		26.3	6.62	129	1565	193	0.15	315	0.54	3.44	195.6	4.8	23.6	58.4	29	23.1	9.09	0.29	46.1	1.24
			28-November-06		27.1	6.70	261	1330	206	<DL	297	0.77	3.47	170.7	4.4	25.9	67.7	39		9.61	0.31	33.8	1.57
			18-January-08		25.9	6.58	310	701	215	1.42	276	<DL	3.16	192.0	3.2	25.4	49.2	53	45.4	9.83	0.44	41.9	2.30
53	Mobarakdi	Black	1-May-04	16.8	26.4	6.65	132	452	202	0.20	13	0.17	5.66	8.2	3.6	11.5	45.1	148	144.2	11.9	0.63	55.2	3.29
			30-January-05		26.6	6.72	111	429	185	0.15	15	0.10	5.87	8.0	3.2	11.0	45.5	160	163.4		0.60	47.9	3.17
54	Mobarakdi	Black	1-May-04	25.9	26.6	6.62	146	877	440	0.15	16	0.24	7.30	35.4	6.4	36.4	91.9	274	258.5	6.98	0.10	48.4	4.11
			30-January-05		26.3	6.73	109	965	441	<DL	10	0.10	6.84	25.1	5.7	30.9	105.6	312	306.3	8.76	0.29	40.4	4.39
			30-November-06		25.4	6.80	285		450	<DL	20	<DL	6.08	32.3	5.0	31.9	90.4	408		6.79	0.10	31.7	3.99
			19-January-08		23.9	6.88	289	750	441	0.44	9	0.60	6.34	28.8	5.2	39.6	109.7	252		6.58	0.31	35.5	5.63
57	Mobarakdi	Black	1-May-04	25.9	26.5	6.67	136	903	459	0.15	12	0.20	7.61	22.3	6.3	36.1	119.6	245	238.5	7.84	0.30	44.6	5.02
			30-January-05		26.2	6.75	104	904	445	0.15	10	0.10	6.90	22.4	5.4	28.7	137.4	259	235.3	7.47	0.30	39.1	4.59
			30-November-06		24.4	6.80	246		445	<DL	8	<DL	6.25	27.2	5.8	30.2	110.6	339		7.42	0.32	29.7	4.09
			19-January-08		23.9	6.88	289	760	450	0.44	8	0.60	6.34	22.8	5.2	39.6	109.7	252	89.9	6.58	0.31	35.5	5.63

adsorbed As(V) was calculated as the difference between the initial and final dissolved As(V). For all experiments with the low As(V) solutions more than 95% of the initial As(V) was adsorbed. Experiments conducted with high As(V) solutions produced similar isotherms for the three sediment samples (Fig. 6). The results indicate that the oxidized sediments have a high capacity to adsorb As(V) (>400–500 mg kg⁻¹). The sediments continued to adsorb As(V) even for the highest As(V) solutions, suggesting that the adsorption sites were not yet saturated. These experiments were only performed for As(V), but if aqueous As(III) is present in water flowing into the oxidized sediments, the adsorption behaviour of As(III) and As(V) onto Fe(III) oxide minerals is similar at pH 6.5–8 (Dixit and Hering, 2003). While the adsorption of As(V) to amorphous Fe(III) oxide minerals is higher than As(III) at low pH (below 5–6), the adsorption of As (III) is greater at a pH higher than 7–8 (Dixit and Hering, 2003; Goldberg, 2002). Therefore, at the near-neutral pH conditions observed in the field it is expected that the oxidized sediments will also have significant capacity to adsorb aqueous As(III). For confirmation it is recommended that the adsorption isotherms for As(III) also be investigated in future studies.

Simulation of the adsorption isotherm experiments with the surface complexation model gave a poor match with the observed data. For all sediment samples, the model under-predicts the adsorption of As (V). For the maximum As(V) solution used, 100 mg L⁻¹, the model under-predicts the adsorbed As by 12–14 times. The model adopted only accounts for adsorption to amorphous Fe(III) oxides (Hfo) and does not consider adsorption sites on Al(III) and Mn(IV) oxides, crystalline Fe(III) oxides nor clay minerals. The poor match indicates that the number of active adsorption sites is greater than that associated with the amorphous Fe(III) oxides and these other minerals may play an important role in the adsorption dynamics. The HNO₃ extractions show that there is a much higher abundance of crystalline compared with amorphous Fe(III) oxides in the sediment (i.e., $Fe_{ox} = 0.09-0.13$ g kg⁻¹ c.f. $Fe_{H-NO3} = 5.1-6.9$ g kg⁻¹). Although the specific surface area and adsorption site density of crystalline Fe(III) oxides is typically lower than for amorphous Fe(III) oxides, this higher abundance may account for the significant number of adsorption sites associated with the crystalline minerals. The model developed has adopted the Hfo surface area and density of weak and strong adsorption sites recommended by Dzombak and Morel (1990). This may vary for the sediments studied and it is recommended that more detailed sediment characterization, is conducted in future investigations including estimation of mineral surface areas and adsorption site density.

3.2.3. Column breakthrough study

The column experiments further illustrate the high capacity of the oxidized sediments to adsorb As. Over the 13 week experimental period, 90–99% of the influent As adsorbed to the sediments. The concentration of As in the influent water was approximately 1900 μg L⁻¹, and throughout the experiment the effluent As concentration ranged from 20–200 μg L⁻¹ (Fig. 7a). The calculated adsorption of As with time is linear suggesting that the adsorption sites were not close to saturation (Fig. 8a). The presence of As in the effluent despite the continued availability of adsorption sites may be associated with flow short-circuiting combined with kinetic constraints on the adsorption process.

The addition of lactose to the replicate columns demonstrates that the availablity of an electron donor decreases the capacity of the oxidized sediments to adsorb As (Fig. 7b). All sediment samples showed a lower adsorption capacity when lactose was present with the adsorption sites for Sample #2 reaching saturation after 9 weeks (Fig. 8b). High dissolved Fe and Mn concentrations in the effluent indicate that the decrease in the sediments' adsorption
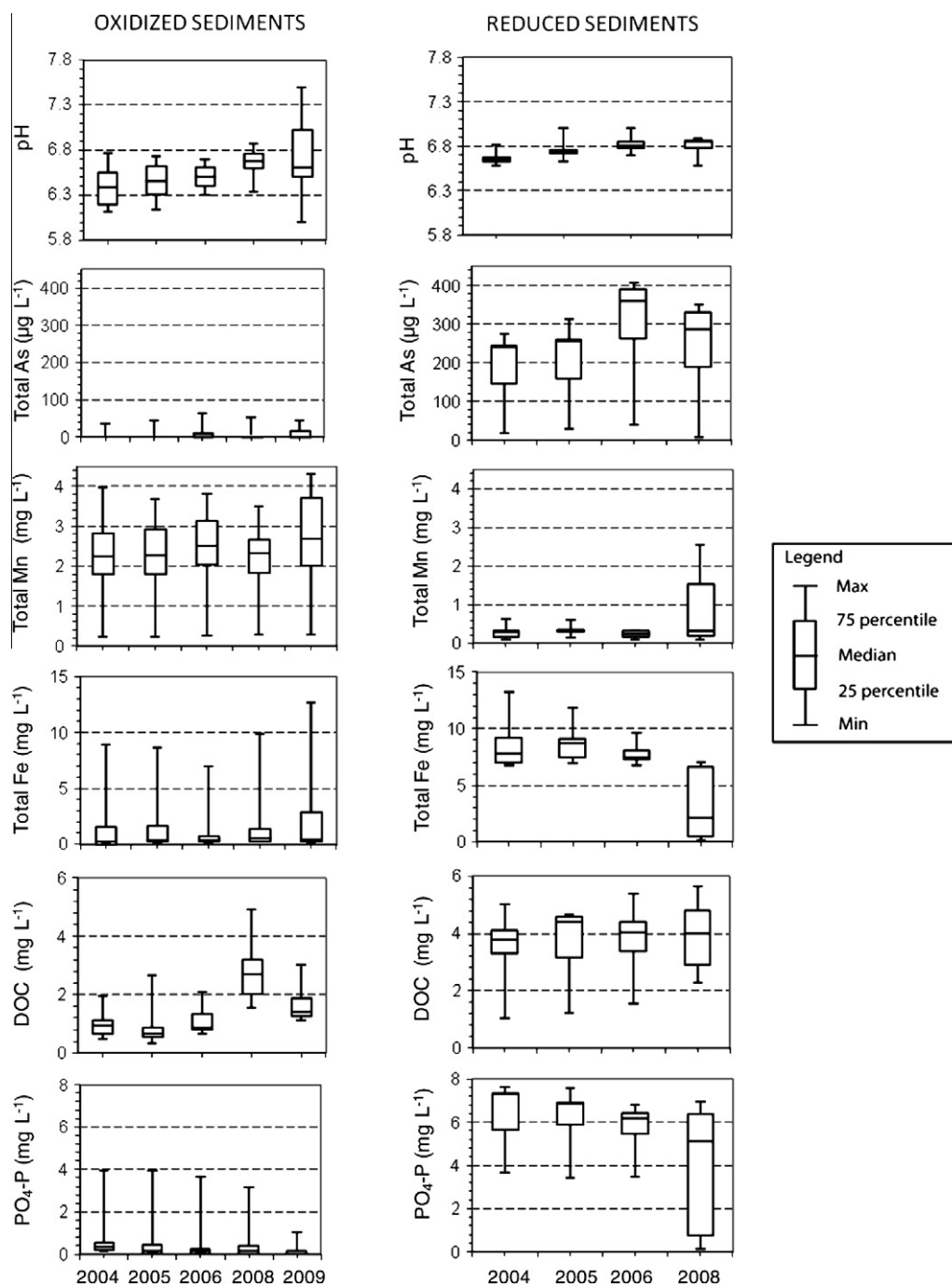
Fig. 3. Box plots showing the temporal variations in major water chemistry parameters (pH, total As, total Mn, total Fe, DOC and PO_4^-P) in the oxidised sediments (left) and reduced sediments (right). Each tube-well water sample was classified as from oxidized or reduced sediment based on the sediment colour at the screened depth (see Table 3).

capacity was due to the reductive dissolution of Fe(III) and Mn(IV) oxides (Fig. 9a and b). In the columns with added lactose, the concentrations of Fe and Mn in the effluent were more than three orders of magnitude greater than for the columns with out added lactose (Fig. 9a and b). Concentrations were highest for Sample #2 indicating that the reductive dissolution of the oxide minerals was greatest in this column. This corresponds with the saturation of adsorption sites observed for this column (Fig. 8b). The effluent concentrations of Ca and Si were also greater for the columns with lactose added, particularly for Sample #2. This suggests that these ions were released as Mn(IV) and Fe(III) oxides were reduced (Fig. 9c and d).

From the redox sequence, reductive dissolution of Mn(IV) oxides should occur in preference to Fe(III) oxides (Appelo and Postma, 2005). While the effluent concentrations indicate that this did occur for Sample #2, for all columns these reactions proceeded concomitantly. This occurs because these processes are microbially mediated and therefore the rates of reaction are affected by the complex consortia of reducing microbes in the sediment. The rates also depend on the relative stability of the specific Fe(III) and Mn(IV) oxides present. Although the reduction of Fe(III) and Mn(IV) oxides adds alkalinity (OH^-) to the solution, the oxidation of lactose adds acidity (H^+). This led to the effluent pH dropping to around 5 (c.f. near-neutral for columns without lactose addition). While
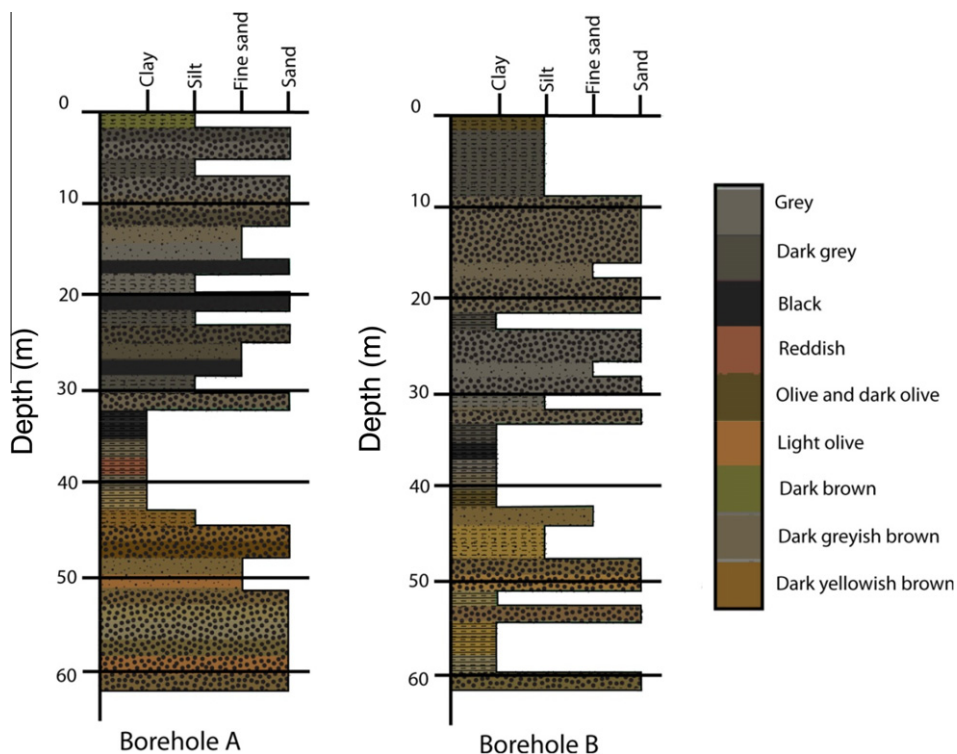
Fig. 4. Lithologs based on washed moist sediment samples from boreholes A and B drilled in North Dighaldi and Mubarakdi villages in November 2006.

Table 4
Results from extraction treatments of the three oxidized sediment samples.

	Oxalate extraction			HNO$_3$ extraction		
	As (mg kg^{-1})	Fe (mg kg^{-1})	Mn (mg kg^{-1})	As (mg kg^{-1})	Fe (mg kg^{-1})	Mn (mg kg^{-1})
Sample #1	<1.3	134.4	9.6	2.1	6940	116
Sample #2	<1.3	118.8	31.2	1.3	5300	153
Sample #3	<1.3	93.6	4.8	2.4	5070	73
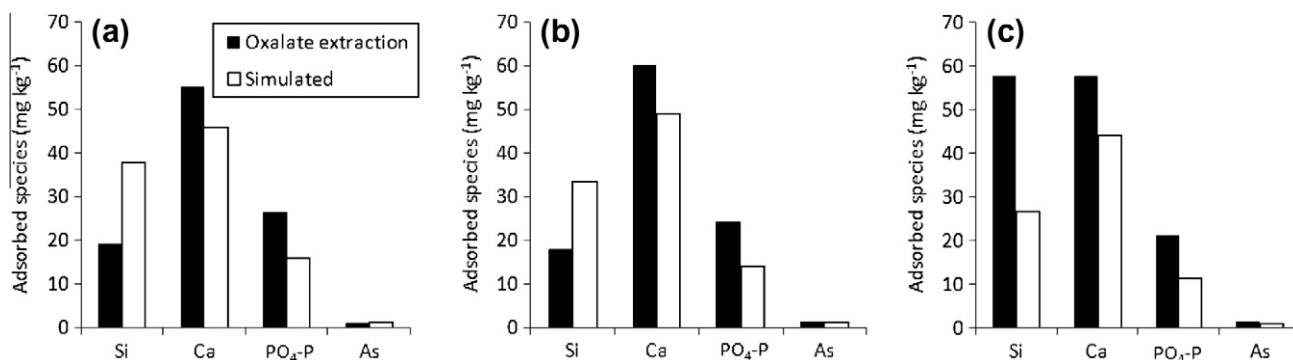
Fig. 5. Distribution of adsorbed species measured from oxalate extractions and simulated using PHREEQC surface complexation model (Table 1). Results are shown for (a) Sample #1, (b) Sample #2, and (c) Sample #3.

decreasing pH has been shown to reduce the adsorption of As(III) to Fe(III) oxides (Dixit and Hering, 2003), the effluent pH decrease does not account for the significant reduction in adsorption capacity observed.

Analysis of the tube-well water demonstrated that DOC concentrations are higher in the reduced sediments compared to the oxidized sediments (Fig. 3). Infiltrating surface waters would also typically also have a much higher organic content (Harvey et al.,

2006). As a result, these experiments show that if groundwater from reduced sediments, or alternatively surface waters, flows into the oxidized sediments, increased DOC availability will enhance the reductive dissolution of oxide minerals triggering the mobilization of As (Bhattacharya et al., 2002b, 2006). The type and reactivity of C used in this column study is different to the complex organic matter that exists in natural aquifer systems. In natural aquifers the reductive dissolution of Fe(III) and Mn(IV) oxides by
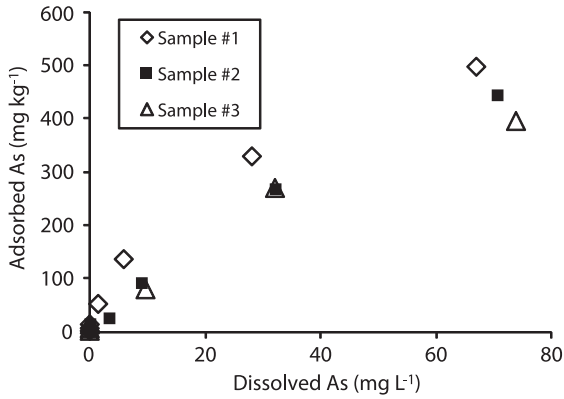
Fig. 6. Measured As adsorption isotherms for Sample #1 (◇), Sample #2 (■) and Sample #3 (△).

DOC will be strongly controlled by kinetics of the microbial processes (McArthur et al., 2004). These kinetics and the type and reactivity of the organic matter available in the sediments needs to be further investigated to more accurately predict (i) the capacity of the oxidized sediments to attenuate dissolved As in the infiltrating water and, (ii) the potential for the dissolution of Fe(III) and Mn(IV) oxides and subsequent release of sediment-bound As, if cross-contamination occurs.

4. Conclusions and recommendations

Batch isotherm and column experiments demonstrate the oxidized sediments in Matlab Region have a high capacity to absorb As. This suggests targeting these sediments for installation of tube-wells may be a simple sustainable solution for delivering As-safe drinking water to the rural communities in areas where oxidized sediments exist at shallow depth. The As adsorption processes however are complex and further investigation is needed to fully assess the risks of contamination including more accurate simulation of the natural conditions in the aquifer.

The isotherm experiments were conducted for As(V) because sampling of tube-wells indicate this is the dominant aqueous redox species in the oxidized sediments. While prior studies have shown that the adsorption behaviour is similar for As(III) at near-neutral pH conditions, it is suggested that the adsorption of As(III) also be examined in future studies as water flowing in from reduced aquifers may have high levels of As(III). Simulations of the experimental isotherms using a surface complexation model under-predict the adsorption capacity of the sediment. This is likely because the model considers adsorption to amorphous Fe(III) oxides only. This indicates that crystalline Fe(III) oxides, Mn(IV) oxides, Al(III) oxides and clay minerals may significantly contribute to the adsorption capacity of the sediment. More detailed characterization of the sediment including quantification of the adsorption site density and mineral surface areas is required.
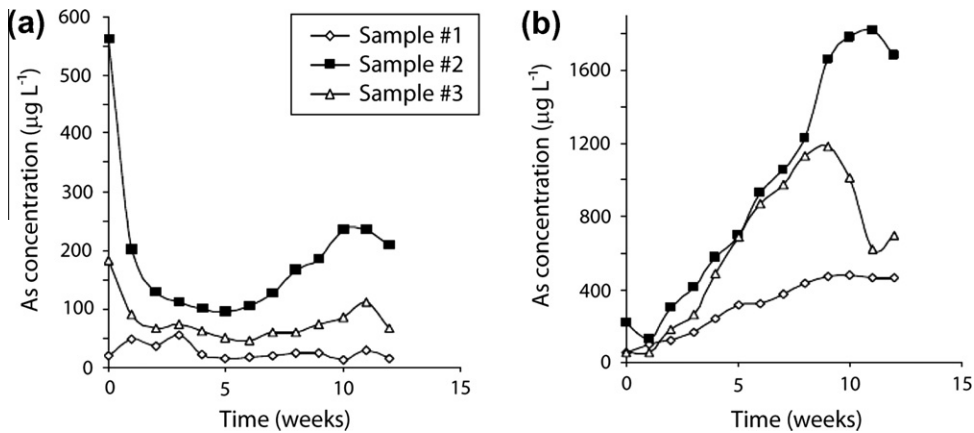

Fig. 7. Measured As concentrations in the effluent for columns (a) without and (b) with lactose added. The legend shown in (a) also applies to (b).
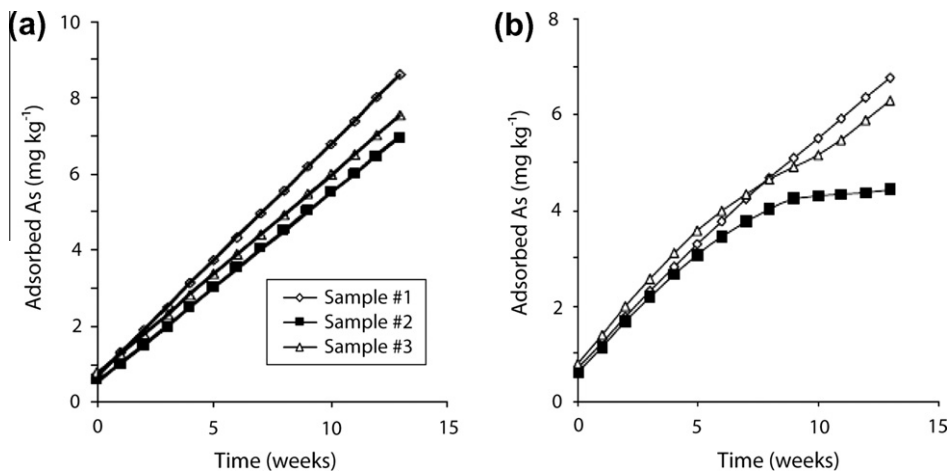

Fig. 8. Calculated amount of As adsorbed to the oxidized sediment in columns (a) without and (b) with lactose added. The legend shown in (a) also applies to (b).
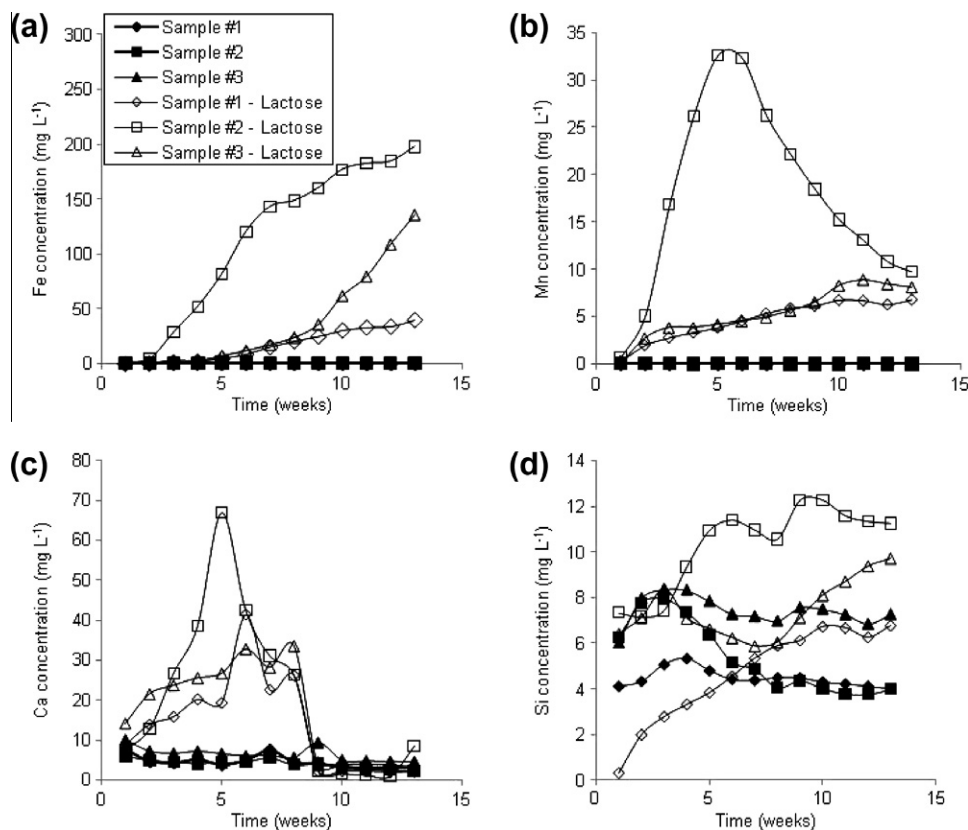
Fig. 9. Measured (a) Fe, (b) Mn, (c) Ca, and (d) Si concentrations in column effluent. The legend shown in (a) also applies to (b–d).

While the capacity of the oxidized sediments to attenuate As was shown to be high, column experiments conducted with lactose added to the influent water showed this capacity may be decreased by high levels of DOC (or other electron donors) in water flowing into the oxidized aquifer layers. Data from the column experiments indicate that the decreased adsorption capacity was due to the reductive dissolution of Fe(III) and Mn(IV) oxides. DOC present in natural aquifers is considerably more complex than lactose which was used here. It is therefore recommended that the reactivity and rate of degradation of natural DOC in the acquifers in the Matlab Region be further investigated with regard to its potential to decrease the adsorption capacity of the oxidized sediments. Finally, to fully evaluate the sustainability of targeting As-safe oxidized aquifers as a source of As-safe water, this experimental work needs to be coupled with long-term and regular monthly monitoring of the water chemistry, including As concentrations, in tube-wells installed in the oxidized sediments.

References

Ahmed, K.M., Bhattacharya, P., Hasan, M.A., Akhter, S.H., Alam, S.M.M., Bhuyian, M.A.H., 2004. Arsenic contamination in groundwater of alluvial aquifers in Bangladesh: an overview. Appl. Geochem. 19, 181–200.

Allison, J.D., Brown, D.S., Novo-Gradac, K.J., 1990. MINTEQA2/PRODEFA2 – A Geochemical Assessment Model for Environmental Systems. US Environmental Protection Agency, Athens, Georgia.

Appelo, C.A.J., Postma, D., 2005. Geochemistry, Groundwater and Pollution, second ed. A.A. Balkema Publishers, Amsterdam, Netherlands.

BGS, DPHE, 2001. Arsenic Contamination of Groundwater in Bangladesh. British Geological Survey, Keyworth.

Bhattacharya, P., Ahmed, K.M., Hasan, M.A., Broms, S., Fogelström, J., Jacks, G., Sracek, O., von Brömssen, M., Routh, J., 2006. Mobility of arsenic in groundwater in a part of Brahmanbaria district, NE Bangladesh. In: Naidu, R., Smith, E., Owens, G., Bhattacharya, P., Nadebaum, P. (Eds.), Managing Arsenic in the Environment: From Soil to Human Health. CSIRO Publishing, Melbourne, Australia, pp. 95–115.

Bhattacharya, P., Bundschuh, J., von Brömssen, M., Hossain, M., Ahmed, K.M., Hoinkis, J., Litter, M., 2010. Arsenic contamination in groundwaters in Bangladesh and options of sustainable drinking water supplies. In: Kabay, N., Bundschuh, J., Hendry, B., Bryjak, M., Yoshizuka, K., Bhattacharya, P., Anac, S. (Eds.), The Global Arsenic Problem: Challenges for Safe Water Production. In: Bundschuh, J., Bhattacharya, P. (Eds.) Interdisciplinary Book Series: Arsenic in the Environment, vol. 2. CRC Press/Balkema, Leiden, The Netherlands, pp. 21–35. ISBN-13: 978-0-415-57521-8.

Bhattacharya, P., Frisbie, S.H., Smith, E., Naidu, R., Jacks, G., Sarkar, B., 2002a. Arsenic in the environment: a global perspective. In: Sarkar, B. (Ed.), Handbook of Heavy Metals in the Environment. Marcel Dekker Inc., New York, USA, pp. 147–215.

Bhattacharya, P., Hasan, M.A., Sracek, O., Smith, E., Ahmed, K.M., von Brömssen, M., Huq, S.M.I., Naidu, R., 2009. Groundwater chemistry and arsenic mobilization in the Holocene flood plains in south-central Bangladesh. Environ. Geochem. Health 31, 23–44.

Bhattacharya, P., Jacks, G., Ahmed, K.M., Khan, A.A., Routh, J., 2002b. Arsenic in groundwater of the Bengal Delta Plain aquifers in Bangladesh. Bull. Environ. Contam. Toxicol. 69, 538–545.

Bivén, A., Häller, S., 2007. Arsenic adsorption behaviour of oxidised aquifers in Matlab Upazila, Bangladesh. Masters Thesis, Royal Institute of Technology, Stockholm, Sweden.

Bundschuh, J., Litter, M., Bhattacharya, P., 2010. Targeting arsenic-safe aquifers for drinking water supplies. Environ. Geochem. Health 32, 307–315.

Dixit, S., Hering, J.G., 2003. Comparison of arsenic(V) and arsenic(III) sorption onto iron oxide minerals: implications for arsenic mobility. Environ. Sci. Technol. 37, 4182–4189.

Dzombak, D.D., Morel, F.M.M., 1990. Surface Complex Modelling. John Wiley & Sons, New York.

Goldberg, S., 2002. Competitive adsorption of arsenate and arsenite on oxides and clay minerals. Soil Sci. Soc. Am. J. 66, 413–421.

Harvey, C.F., Ashfaque, K.N., Yu, W., Badruzzaman, A.B.M., Ali, M.A., Oates, P.M., Michael, H.A., Neumann, R.B., Beckie, R., Islam, S., Ahmed, M.F., 2006. Groundwater dynamics and arsenic contamination in Bangladesh. Chem. Geol. 228, 112–136.

Hasan, M.A., Ahmed, K.M., Sracek, O., Bhattacharya, P., von Brömssen, M., Broms, S., Fogelström, J., Mazumder, M.L., Jacks, G., 2007. Arsenic in shallow groundwater of Bangladesh: investigations from three different physiographic settings. Hydrogeol. J. 15, 1507–1522.

Hasan, M.A., von Brömssen, M., Bhattacharya, P., Ahmed, K.M., Sikder, A.M., Jacks, G., Sracek, O., 2009. Geochemistry and mineralogy of shallow alluvial aquifers in Daudkandi upazila in the Meghna flood plain, Bangladesh. Environ. Geol. 57, 499–511.

Jakariya, M., von Brömssen, M., Jacks, G., Chowdhury, A.M.R., Ahmed, K.M., Bhattacharya, P., 2007. Searching for sustainable arsenic mitigation strategy in Bangladesh: experience from two upazilas. Int. J. Environ. Pollut. 31, 415–430.

Jonsson, L., Lundell, L., 2004. Targeting Safe Aquifers in Regions with Arsenic-rich Groundwater in Bangladesh: Case Study in Matlab Upazila, Minor Field Studies, vol. 277. Swedish University of Agricultural Sciences, Uppsala.

Kapaj, S., Peterson, H., Liber, K., Bhattacharya, P., 2006. Human health effects from chronic arsenic poisoning – a review. J. Environ. Sci. Health Part A 41, 2399–2428.

McArthur, J.M., Banerjee, D.M., Hudson-Edwards, K.A., Mishra, R., Purohit, R., Ravenscroft, P., Cronin, A., Howarth, R.J., Chatterjee, A., Talukder, T., Lowry, D., Houghton, S., Chadha, D.K., 2004. Natural organic matter in sedimentary basins and its relation to arsenic in anoxic ground water: the example of West Bengal and its worldwide implications. Appl. Geochem. 19, 1255–1293.

Meng, X., Korfiatis, G.P., Christodoulatos, C., Bang, S., 2001. Treatment of arsenic in Bangladesh well water using a household co-precipitation and filtration system. Water Res. 35, 2805–2810.

Naidu, R., Bhattacharya, P., 2009. Arsenic in the environment-risks and management strategies. Environ. Geochem. Health 31 (Supp. 1), 1–8.

Nath, B., Chakraborty, S., Burnol, A., Stüben, D., Chatterjee, D., Charlet, L., 2009. Mobility of arsenic in the sub-surface environment: an integrated hydrogeochemical study and sorption model of the sandy aquifer materials. J. Hydrol. 364, 236–248.

Parkhurst, D.L., Appelo, C.A.J., 1999. User's guide to PHREEQC (version 2) – a computer program for speciation, batch-reaction, one dimensional transport, and inverse geochemical calculations. US Geol. Surv. Water-Resour. Invest. Rep. 99-4259.

Polizzotto, M.L., Harvey, C.F., Sutton, S.R., Fendorf, S., 2005. Processes conducive to the release and transport of arsenic into aquifers of Bangladesh. PNAS 102, 18819–18823.

Polya, D., Charlet, L., 2009. Rising arsenic risk? Nat. Geosci. 2, 383–384.

Rahman, M.M., Naidu, R., Bhattacharya, P., 2009. Arsenic contamination in groundwater in the Southeast Asia region. Environ. Geochem. Health 31 (Supp. 1), 9–21.

Sharif, M.U., Davis, R.K., Steele, K.F., Kim, B., Hays, P.D., Kresse, T.M., Fazio, J.A., 2008. Distribution and variability of redox zones controlling spatial variability of arsenic in the Mississippi River Valley alluvial aquifer, southeastern Arkansas. J. Contam. Hydrol. 99, 49–67.

SIS, 1996. Water quality. Determination of alkalinity, part 2:Determination of Carbonate Alkalinity. Swedish Standards Institution, (Ss-EN ISO 9963–2), Stockholm.

Stollenwerk, K.G., Breit, G.N., Welch, A.H., Yount, J.C., Whitney, J.W., Forster, A.L., Uddin, M.N., Majumder, R.K., Ahmed, N., 2007. Arsenic attenuation by oxidised sediments in Bangladesh. Sci. Total Environ. 379, 133–150.

Swedlund, P.J., Webster, J.G., 1999. Adsorption and polymerization of silicate acid on ferrihydrite, and its effect on adsorption. Water Res. 33, 3413–3422.

van Geen, A., Ahasan, H., Horneman, A.H., Dhar, R.K., Zheng, Y., Hussain, I., Ahmed, K.M., Gelman, A., Stute, M., Simpson, H.J., Wallace, S., Small, C., Parvez, F., Slakovich, V., Lolacono, N.J., Becker, M., Cheng, Z., Momtaz, H., Shahnewaz, M., Seddique, A.A., Graziano, J., 2002. Promotion of well-switching to mitigate the current arsenic crisis in Bangladesh. Bull. WHO 80, 732–737.

van Geen, A., Rose, J., Thoral, S., Garnier, J.M., Zheng, Y., Bottero, J.Y., 2004. Decoupling of As and Fe release to Bangladesh groundwater under reducing conditions. Part II: evidence from sediment incubations. Geochim. Cosmochim. Acta 68, 3475–3486.

von Brömssen, M., Jakariya, M., Bhattacharya, P., Ahmed, K.M., Hasan, M.A., Sracek, O., Jonsson, L., Lundell, L., Jacks, G., 2007. Targeting low-arsenic aquifers in Matlab Upazila, Southeastern Bangladesh. Sci. Total Environ. 379, 121–132.

von Brömssen, M., Larsson, S.H., Bhattacharya, P., Hasan, M.A., Ahmed, K.M., Jakariya, M., Sikder, M.A., Sracek, O., Bivén, A., Dousova, B., Patriarca, C., Thunvik, R., Jacks, G., 2008. Geochemical characterisation of shallow aquifer sediments of Matlab Upazila, Southeastern Bangladesh – implications for targeting low-As aquifers. J. Contam. Hydrol. 99, 137–149.

WHO, 2004. Guidelines for Drinking-water Quality, third ed. Recommendations, vol. 1. World Health Organization, Geneva.

Zheng, Y., Stute, M., van Green, A., Gavrieli, I., Dhar, R., Simpson, H.J., 2004. Redox control of arsenic mobilization in Bangladesh groundwater. Appl. Geochem. 19, 201–214.